104 (2025) 104517

Contents lists available at ScienceDirect

Poultry Science

journal homepage: www.elsevier.com/locate/psj

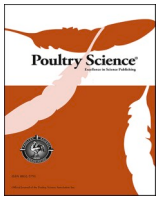

Utilization of edible poultry slaughter residues: A chicken-liver hydrolysate with glucose-lowering ability and upregulating glycogenesis in type II diabetes

Yi-Ling Lin [a,b], Yu-Pei Chen [a], Sheng-Yao Wang [a], Yi-Feng Kao [c], Chompunut Lumsangkul [d], Yi-Chen Chen [a,e,*]

[a] Department of Animal Science and Technology, National Taiwan University, Taipei City 106037, Taiwan
[b] Undergraduate and Graduate Programs of Nutrition Science, National Taiwan Normal University, Taipei City 116059, Taiwan
[c] Seafood Technology Division, Fisheries Research Institute, Ministry of Agriculture, Keelung City 202008, Taiwan
[d] Department of Animal Science, National Chung-Hsing University, Taichung City 402202, Taiwan
[e] Master Program in Global Agriculture Technology and Genomic Science, International College, National Taiwan University, Taipei City 106319, Taiwan

ARTICLE INFO

Keywords:
Chicken-liver hydrolysate
In-vitro experiment
db/db mice
Type II diabetes
Glycogenesis

ABSTRACT

Approximately 10,000 metric tons of broiler livers are yielded every year in Taiwan. However, due to unpleasant odor and health concern, these livers are typically discarded as waste in the slaughtering stream in most developed or developed countries. In alignment with global agrocycle policies, a biofunctional chicken-liver hydrolysate (CLH) has been developed. This study was to investigate the effects of CLHs on glucose homeostasis and complications in type II diabetes. Insulin resistance was induced in liver (FL83B) and muscle (C2C12) cells using 30 and 20 ng TNF-α/mL, respectively, resulting in decreased glucose uptake and lower expressions of IRβ, p-Akt/Akt, and p-GSK3/GSK. CLH supplementation significantly upregulated ($p<0.05$) glucose uptakes and these proteins. In db/db mice, CLH supplementation improved insulin resistance, as shown by OGTT assay, HOMA-IR value and serum glucose levels, while also reducing serum lipids and liver damage indices ($p<0.05$). Additionally, CLH ameliorated ($p<0.05$) decreased hindlimb-gastrocnemius weight, and liver lipid contents, oxidative stress (sera and liver) and inflammatory cytokines. Increased glycogen accumulation was visualized in PAS-stained liver and hindlimb tissues of db/db mice supplemented with CLHs, consistent with upregulated glycogenesis in TNF-α-induced liver and muscle cells through the IRβ-Akt-GSK3 pathway. These findings suggest CLH may offer a mitigation against hyperglycemia and associated complications in type II diabetes, while also highlighting a sustainable solution for utilizing poultry slaughter residues.

Introduction

Recently, a circular economic model that uses agricultural wastes, by-products, and co-products via innovative technologies and business practices is encouraged worldwide. For example, approximately 1.3 billion tons of waste were generated annually in Europe, where 700 million tons are from agricultural residues or waste (Toops et al., 2017). Wu and Chen (2022) proposed that protein hydrolyzation could offer a possible application for maximizing utilization of animal by-products. In Taiwan, due to several reasons, i.e. nutrition, affordability, tenderness, taste etc., poultry has been the top one meat consumption per capita among all meat categories while approximately 418.6 million metric tons of broilers were slaughtered in 2022, yielding over a production of 10,000 metric tons of broiler livers yearly (Ministry of Agriculture, Executive Yuan, Taiwan, 2023). Unfortunately, broiler's livers are not preferable to consumers due to their unfavored flavor and health concern for consumers. Our team has successfully developed a chicken-liver hydrolysate (CLH) via a patented hydrolyzation technology (Chen et al., 2018) with antioxidant (Chou et al., 2014), hypolipidemic and cardioprotective effects (Yang et al., 2014; Wu et al., 2020); meanwhile, hepatoprotection against chronic alcohol consumption (Lin et al., 2017), liver fibrogenesis (Chen et al., 2017), and long-term high-fat diet (Wu et al., 2021).

Globally, approximately 573 million people have been diagnosed

* Corresponding author.
E-mail address: ycpchen@ntu.edu.tw (Y.-C. Chen).

https://doi.org/10.1016/j.psj.2024.104517
Received 17 September 2024; Accepted 4 November 2024
Available online 7 November 2024

with diabetes, a number expected to rise to 783 million by 2045 (Ahmad et al., 2022). According to statistics from Ministry of Health and Welfare, Taiwan (2023), the diabetes always lists in 10 leading causes of death, ranking the 5th position. In 2022, the number of deaths attributed to diabetes increased by 7.3% compared to 2021. Type II diabetes, which accounts for 90% of cases, is primarily caused by an insulin resistance (Ahmad et al., 2022). In the glucose homeostasis, liver and muscle play an important role to uptake glucose by an insulin stimulation (Chadt and Al-Hasani, 2020). However, the insulin resistance results in impairing glycogenesis, glycogenolysis and gluconeogenesis, affecting the expression of key enzymes like glucose-6-phosphatase catalytic subunit (G6PC) and phosphoenolpyruvate carboxykinase 1 (PCK-1) in gluconeogenesis or insulin receptor β (IRβ)-Akt-glycogen synthase kinase-3 (GSK3) pathways in glycogenesis (Petersen and Shulman, 2018). In the glycogenesis, an insulin stimulates an activation of IRs, Akt phosphorylation and then inactivates GSK3 to phosphorylated GSK, resulting in the dephosyphorylation of glycogen synthase (GS). This, in turn, increases glycogen synthesis. Huang et al. (2016) indicated that the ameliorative effects of gallic acid on diabetes results from downregulation of hepatic gluconeogenesis-related proteins, such as fructose-1,6-bisphosphatase, and upregulation hepatic glycogen synthase and glycolysis-related proteins, such as hexokinase, phosphofructokinase, and aldolase. Additionally, supplementation with saponin and resveratrol also showed the hypoglycemic effect via enhancing glycogenesis in livers and myotubes (Lu et al., 2016; Park et al., 2020). Therefore, targeting glycogenesis might be a potential approach to improve insulin resistance (Zhu et al., 2021; Wang et al., 2022). To our knowledge, there are only a few studies on the benefits of protein hydrolysates in combating insulin resistance by enhancing glycogenesis.

Streptozotocin (STZ) is a specific cytotoxin that targets pancreatic beta cells, leading to reduced insulin secretion and resulting in type I diabetes (Furman, 2021). Recently, we also demonstrated that CLH supplementation lowers blood glucose by increasing glucose transporter 4 (GLUT4) protein expressions in the brains, livers, and muscles of streptozotocin (STZ) induced mice which is (Yeh et al., 2022). Meanwhile, CLH supplementation improved memory (water maze) and alternation behavior (Y maze) in STZ-induced mice by reducing contracted neuron bodies in the hippocampus, decreasing β-amyloid deposition in the dentate gyrus, lowering AGE accumulation, and downregulating apoptosis-related proteins in the brain. Based on the free amino-acid and imidazole-ring dipeptide profile in our CLHs (Wu et al., 2020), several amino acids. i.e. taurine (Inam-U-Llah et al., 2018), glycine (Li et al., 2019a), and branched-chain amino acids (BCAAs) (Zhu et al., 2021), as well as an imidazole-ring dipeptides, i.e. anserine inside CLHs have been identified as hypoglycemic effects (Peters et al., 2018). Moreover, Liao et al. (2023) reported that a 9-week treatment of pea protein hydrolysates reduced fasting blood glucose level and improve glucose tolerance in high-fat diet and STZ treated mice via a suppression of the gluconeogenic pathway. To identify glucose-lowering effects against type II diabetes (insulin resistance), we proposed that bioactive components derived from broiler slaughter residues, specifically pepsin-digested CLHs, could improve insulin resistance in type II diabetes. Besides, it has been proven that a tumor necrosis factor-alpha (TNF-α) induction can successfully induce the insulin resistance in liver (Huang et al., 2009) and muscle (Lee et al., 2011) models. For this purpose, *in vitro* (liver and muscle cells) and *in vivo* (db/db mice) experiments were set up to prove this biofunctionality; meanwhile, the glycogenesis (IRβ-Akt-GSK3 pathway) on glucose regulation was elucidated as well.

Materials and methods

Preparation of pepsin-digested chicken-liver hydrolysates (CLHs) and free amino acid profile, manganese, and selenium contents

According to the manufacturing procedure from a patent of Chen et al. (2022), CLHs was produced in a pilot-scale facility via an enzyme digestion. Briefly, the chicken livers with Certified Agriculture Standards (CAS) were transported to our laboratory under -20°C. They were hydrolyzed by pepsin at pH 2.0 for 2 h and immediately heated at 95°C for 30 min to stop the hydrolyzation. After that, the clear supernatant was collected and freeze-dried to obtained CLH powder. The free amino acid profile in CLH powder was analyzed by amino acid analyzer (model L8800, Hitachi High-Technologies Co., Tokyo, Japan) in Food Industry Research and Development Institute (FIRDI, HsinChu City, Taiwan). First, CLHs were ashed (550°C, 6 h) and dissolved in 2 mL of 70% (w/v) nitric acid. Then magnesium (Mg), manganese (Mn) and selenium (Se) contents in CLHs were analyzed by using inductively coupled plasma optical emission spectrometry (ELEMENT 2* ICP-MS; Thermo Fisher Scientific Inc., MA, USA) in Experiment Station Chemical Laboratories of National Animal Industry Foundation, Pingtung, Taiwan. The amino acid profile, Mg, Mn, and Se contents in CLHs were demonstrated in Suppl. Table 1.

In vitro experiment

FL83B and C2C12 cell culture

Both FL83B (BCRC 60325) and C2C12 cells (BCRC 60083) were obtained from the Bioresource Collection and Research Center of Food Industry Research and Development Institute, Hsinhu City, Taiwan. FL83B cells are a normal hepatocyte cell line derived from mouse livers. FL83B cells were cultured in Nutrient Mixture F12K media (Gibco, Grand Island, NY, USA) with 10% fetal bovine serum (FBS, PAN Biotech UK Ltd., Wimborne Dorset, UK), 1% penicillin streptomycin solution (PAN Biotech UK Ltd.), and 1.5 g/L sodium bicarbonate at 37°C with 5% CO_2. C2C12 cells are derived from mouse muscle myoblast of normal adult C3H mouse leg muscle. C2C12 cells were cultured in Dulbecco's Modified Eagle media (DMEM, Simply Co., Ltd., Kaohsiung City, Taiwan) with 10% fetal bovine serum (FBS, PAN Biotech UK Ltd.), 1% penicillin streptomycin solution (PAN Biotech UK Ltd.), and 1.5 g/L sodium bicarbonate at 37°C with 5% CO_2. First, differentiation of C2C12 cells was determined by myotube formation under the microscopic observation. Differentiated C2C12 cells were used for further experiment. The survival rate (Cell Counting Kit-8; Enzo Life Science, Inc., Farmingdale, NY, USA) and lactate dehydrogenase (LDH) leakage (LDH-Cytotoxicity Colorimetric Assay Kit II; BioVision Inc., Milpitas, CA, USA) of FL83B and C2C12 cells affected by CLHs (FL83B cells: 0, 5, 25, 50, and 75 μg/mL; C2C12 cells: 0, 5, 10, 25, and 50 μg/mL) were assayed according to the commercial manuals, respectively. The quantities of FL83B and C2C12 cells in assays were 2×10^4 cells/well in a 96-well plate and 2.5×10^3 cells/well in a 24-well plate, respectively. Neither relative survival rate nor LDH leakage of FL83B and C2C12 cells was affected by CLH concentrations below 75 and 50 μg/mL, respectively (Suppl. Fig. 1).

Insulin resistance induction and the glucose uptake assay

The FL83B and C2C12 cells were treated various CLH levels for 12 h, and then new media were changed. The insulin resistances in FL83B and C2C12 were induced by 30 ng/mL TNF-α (Huang et al., 2009) and 20 ng/mL TNF-α (Lee et al., 2011) for 5 h, respectively. The glucose uptake assays of FL83B and C2C12 cells were determined based on the measurement of NADPH production from 2-deoxyglucose-6-phosphatase (2-DG6P, a glucose analogue) uptake by cells in an insulin induction (500 ng/mL; Insulin human, Sigma Sigma-Aldrich Co., St. Louis, MO, USA) with a Glucose Uptake Assay kit (Colorimetric, Abcam plc, Cambridge, England). Briefly, the detached normal or insulin resistant cells were suspended in Krebs-Ringer-Phosphate-Hepes (KRRH) buffer (HEPES: 20 mM; KH_2PO4: 5 mM; $MgSO_4$: 1 mM; NaCl: 136 mM; KCl: 4.7 mM) (Product Code: TS1152, HiMedia Laboratories Pvt. Ltd., Maharashtra, India) containing 2% BSA (Sigma-Aldrich Co.). After 40-min reaction, the buffer was removed, and cells were washed by phosphate buffered saline for thrice. Then, cells were divided into two groups,

blank and insulin stimulated groups. The cell homogenate of bank group was lysed by extraction buffer for further analyses. The insulin stimulated groups were resuspended in KRRH buffer containing 2% BSA (Sigma-Aldrich Co.) and 500 nM insulin. After 20 min, 10 μL 2-DG6P solution was then added to insulin stimulated groups with or without CLHs. Then the NADPH production in blank and insulin stimulated groups with or without CLHs were assayed by using Glucose Uptake Assay kit. The relative glucose uptake of groups was calculated based on group without TNF-α and CLHs, which was set to 1.0.

Western blotting

Protein from treated FL83B and C2C12 cells from each treatment was extracted by RIPA buffer (Merck & Co., Inc., Kenilworth, NJ, USA) with proteinase inhibitor cocktail (cOmplete™, mini, EDTA-free Protease inhibitor cocktail, Roche, Basel, Switzerland), and then protein samples were mixed with Laemmli buffer and boiled at 95°C for 10 min. The procedures for western blotting were according to previous report (Wu et al., 2021). The antibodies used in this study were IRβ (1:1000 dilution; #3025, Cell Signaling Technology Inc., Danvers, NJ, USA), total Akt (1:1000 dilution; PA1-22099, Thermo Fisher Scientific Inc., Waltham, MA, USA) and p-Akt (Thr308) (1:1000 dilution; #9275, Cell Signaling Technology Inc.), GSK3 (1:1000 dilution; #9315, Cell Signaling Technology Inc.) and p-GSK3 (Ser9) (1:1000 dilution; #9323, Cell Signaling Technology Inc.), and β-actin (1:5000 dilution; #3700, Cell Signaling Technology Inc.). The secondary antibody was goat anti-rabbit IgG (1:5000 dilution; #31460, Thermo Fisher Scientific Inc.). Densitometry illustrations were performed by using Image Lab software (BioRad, Hercules, CA, USA). Image J software (National Institutes of Health) was used to quantify the optical density of protein bands with the value of the β-actin band as a reference. The relative folds of IRβ, and ratios of p-Akt/Akt and p-GSK3 (Ser9)/GSK3 of other groups were expressed relatively to that of the group cells without TNF-α and CLHs, which was set to 1.0.

In vivo experiment

Animals and treatments

Thirty-two male C57BLKS/J-*db/db* mice (db/db mice) and 8 C57BLKS/J-m^+/m^+ male mice (m^+/m^+ mice) with 4 weeks old were purchased from National Laboratory Animal Center (Taipei City, Taiwan), and acclimatized for one week before the experiment starts. Mice were housed in an animal room (24°C, 60% R.H., light-dark cycle: 12h/12h) and fed with chow diet (LabDiet® 5001, PMI Nutrition International/Purina Mills LLC, Richmond, IN, USA) and distilled water throughout the experimental period. C57BLKS/J-m^+/m^+ mice were assigned to the Control group which orally fed with 10 mL ddH_2O/Kg BW while db/db mice were randomly divided to the following 4 groups: 1) db/db group: Orally fed with 10 mL ddH_2O/Kg BW; (2) db/db mice+CLH 1X group: Orally fed with 85 mg CLH/Kg BW in 10 mL ddH_2O/Kg BW; (3) db/db mice+CLH 2X group: Orally fed with 170 mg CLH/Kg BW in 10 mL ddH_2O/Kg BW; (4) db/db mice+ACTOS group: Orally fed with 24.67 mg ACTOS®/Kg BW in 10 mL ddH_2O/Kg BW. The oral supplementation was applied at 8am every day, and CLH dosages were according to our previous report (Wu et al., 2021). Two mice were caged with ear tag (No. 1 and 2). The experiment lasted for 84 days. ACTOS® was purchased from Takeda Pharmaceutical Co, LTD. (Tokyo, Japan) [30 mg pioglitazone hydrochloride/tablet (approx. 120 mg per tablet)] and used as a positive control agent (Yeh et al., 2022). The dosage of ACTOS® was calculated according to the conversion from the hypoglycemic effects of pioglitazone-hydrochloride dosage in adults (one tablet/day) (Yeh et al., 2022). Average daily feed and water intakes were calculated as volumes of diet and water consumption on per mouse daily basis, respectively. All mice were fasted overnight (8h) before euthanized by CO_2 in the final day of experiment. The initial and final body weights were recorded. The heart, liver, spleen, kidney, subcutaneous and abdominal (perirenal, mesenteric, and epididymal) adipose tissues and hindlimb gastrocnemius tissues from each mouse were removed, weighed individually, and then stored at -80°C for further analyses. The animal use and protocol were approved by the National Taiwan University Institution Animal Care and Use Committee (IACUU Approval No: NTU106-EL-00092).

Oral glucose tolerance test (OGTT)

The OGTT assay (one g glucose/Kg BW, oral gavage) was executed in the 78th day in the experimental period. The diet was completely removed 8 h before starting the assay. The serum glucose level per mouse was detected in 0, 30, 60, 90 and 120 min after the mice were orally administered with one g glucose/Kg BW. Blood samples were collected by orbital sinus and placed at room temperature for clotting, and then centrifuged (3,000 xg), 4°C for 15 min to obtain sera. Serum glucose were measured by a commercial kit (Randox Laboratories Ltd., Antrim, UK) while the serum glucose level under the curve (AUC) was calculated by a trapezoidal rule (Wu et al., 2021; Yeh et al., 2022).

Serum biochemical values and antioxidant capacities, as well as liver lipids, antioxidant capacities and cytokines

Before sacrificed on the 84th day, mice were fasted overnight, and blood samples were collected via orbital sinus. After clotting for one h at room temperature, the sera were obtained from blood samples by centrifugation at 3,000 xg, 4°C for 15 min (Centrifuge, 3700, Kubota Co. Tokyo, Japan) and then stored at -20°C for future analyses. Serum glucose, triglyceride, total cholesterol, aspartate aminotransferase (AST), and alanine aminotransferase (ALT) were analyzed by using commercial enzymatic kits (Randox Laboratories Ltd.). The serum insulin (Mouse Insulin ELISA, Mercodia Inc., Sylveniusgatan, Uppsala, Sweden) while dipeptidyl peptidase 4 (DPP4) activity (Abcam plc) and glucagon-like peptide 1 (GLP1) levels (RayBiotech Life, Inc., Pottstown, PA, USA) were measured by using commercial enzymatic kits. HOMA-IR was calculated as formula: HOMA-IR= fasting glucose (mmole/L) x fasting insulin (mU/L)/22.5 (Liu et al., 2020). The liver homogenate and its protein levels were prepared and measured according to the procedures from Wu et al. (2021). The antioxidant capacities in sera (TBARS and TEAC) and livers (TBARS, reduced GSH, TEAC, SOD, catalase, and GPx) were also assayed according to the procedures from our previous reports (Chen et al., 2020, 2021) while liver lipids (triglyceride and cholesterol) and cytokines (IL-1β, IL-6, and TNF-α) were also assayed according to previous methods and kits described by Chen et al. (2021).

Histological examination

First, the liver and hindlimb tissues were placed in a 3.7% formaldehyde solution up to 48 h and then kept dehydrated in graded alcohol (30, 50, 75, and 95%), cleared in xylene, and embedded in paraffin wax. The liver blockers were sliced in 5-mm thickness by using a microtome, deparaffinized in xylene, dehydrated in graded alcohol, and stained with hematoxylin and eosin (H&E) solution. Regarding the observation of glycogen deposition in liver and hindlimb tissues, the tissue slices were stained with periodic acid-Schiff reagent (PAS). Photomicrographs were taken by using a Leica DM500 microscope (Leica Microsystems, Singapore) with an IHD-4600 camera system (Sage Vision Co. Ltd., New Taipei City, Taiwan) and ToupView 3.7 software (ToupTek Co. Ltd., Hangzhou, China). According to H&E stained observation, the histologic grade and stage of hepatic steatosis were then determined according to a report by Dixon et al. (2004). Additionally, this hepatic steatosis score is a 5-grade system (0: no steatosis, 1: 5% of hepatocytes affected; 2: 5 to 25% of hepatocytes affected; 3: 25 to 75% of hepatocytes affected; 4: 75% of hepatocytes affected).

Statistical analysis

The experiment was conducted by using a completely randomized design (CRD). To control for potential inflation of Type I error, data were

Table 1
Effects of chicken-liver hydrolysates (CLHs) on growth performance, organ and adipose-tissue weights, serum biochemical values, and liver lipids of experimental mice.

	Control	db/db	db/db+CLH 1X	db/db+CLH 2X	db/db+ACTOS
Initial body weight (g)	21.33 ±0.21b	32.35 ±0.54a	32.73 ±0.36a	32.48 ±0.81a	32.38 ±0.54a
Final body weight (g)	25.53 ±0.37c	37.46 ±0.76ab	36.34 ±1.11ab	34.00 ±1.95b	39.11 ±1.78a
Feed intake (g/mouse/day)	2.99 ±0.10b	7.15 ±0.25a	7.24 ±0.21a	7.37 ±0.32a	7.37 ±0.34a
Water intake (mL/mouse/day)	4.42 ±0.40c	25.30 ±0.55a	17.39 ±0.84b	17.96 ±1.21b	15.40 ±1.41b
	Organ weights (g/mouse)				
Heart	0.11 ±0.00a	0.11 ±0.00a	0.12 ±0.00a	0.11 ±0.01a	0.12 ±0.00a
Liver	1.04 ±0.02c	2.15 ±0.07a	1.90 ±0.04ab	1.80 ±0.13b	1.98 ±0.12ab
Spleen	0.06 ±0.00a	0.06 ±0.00a	0.06 ±0.00a	0.06 ±0.01a	0.06 ±0.00a
Kidney	0.30 ±0.02b	0.47 ±0.02a	0.42 ±0.02a	0.44 ±0.03a	0.44 ±0.02a
Subcutaneous adipose tissue	0.52 ±0.06c	4.99 ±0.36a	4.58 ±0.22a	3.33 ±0.37b	4.81 ±0.41a
Abdominal adipose tissue	1.78 ±0.07c	4.24 ±0.16a	3.49 ±0.13b	3.08 ±0.12b	4.03 ±0.30a
Perirenal adipose tissue	0.43 ±0.01c	0.83 ±0.04a	0.63 ±0.05b	0.63 ±0.04b	0.76 ±0.05a
Mesenteric adipose tissue	0.63 ±0.03c	1.17 ±0.08a	0.86 ±0.05b	0.73 ±0.06bc	1.17 ±0.10a
Epididymal adipose tissue	0.72 ±0.03c	2.24 ±0.05a	2.00 ±0.04ab	1.73 ±0.21b	2.11 ±0.17a
Gastrocnemius	1.20 ±0.05a	0.50 ±0.03c	0.80 ±0.05b	0.80 ±0.04b	0.78 ±0.06b
	Serum biochemical values				
Glucose (mmol/L)	9.75 ±0.35c	31.42 ±0.71a	20.04 ±1.35b	23.19 ±2.04b	21.73 ±1.68b
Insulin (mU/L)	11.99 ±0.13a	11.53 ±0.11a	11.63 ±0.23a	10.97 ±0.18b	10.73 ±0.22b
HOMA-IR	5.20 ±0.20c	16.37 ±0.33a	10.37 ±0.73b	11.25 ±0.57b	10.35 ±0.54b
Triglyceride (mg/dL)	58.68 ±3.11d	270.50 ±10.74a	210.64 ±9.35b	208.11 ±11.32bc	182.45 ±9.26c
Total cholesterol (mg/dL)	97.18 ±2.35d	201.11 ±6.61a	135.33 ±5.14c	131.29 ±4.57c	181.84 ±7.91b
AST (U/L)	111.26 ±9.90c	266.82 ±12.74a	144.86 ±14.29bc	147.27 ±16.06b	176.96 ±8.45b
ALT (U/L)	102.80 ±6.32c	211.27 ±19.15a	134.87 ±10.88bc	137.96 ±15.75bc	156.65 ±11.60b
DPP4 (U/mL)	0.64 ±0.02c	0.80 ±0.03a	0.77 ±0.04ab	0.67 ±0.05bc	0.62 ±0.06c
GLP1 (ng/mL)	207.76 ±10.22a	126.77 ±9.91c	155.22 ±9.36bc	180.02 ±9.77ab	144.88 ±12.74c
	Liver lipids				
Triglyceride (mg/g liver)	12.45 ±1.06c	29.80 ±1.99a	21.82 ±1.73b	21.69 ±2.06b	25.33 ±1.71ab
Cholesterol (mg/g liver)	4.15 ±0.67d	9.03 ±0.74a	6.81 ±0.48bc	6.34 ±0.85c	8.59 ±0.43ab

*Data are given as mean±SEM (n=8). Mean values without a common letter indicate a significant difference ($p<0.05$).

analyzed by using analysis of variance (ANOVA) at a significance level of 0.05. Upon finding significant differences among groups, post-hoc comparisons between treatments were further examined by using the least significant difference (LSD) test. All analyses were performed with SAS 9.4 software (SAS Institute Inc., Cary, NC, USA, 2002).

Results

Glucose uptake and protein expressions related to IRβ-Akt-GSK3 pathway in FL83B and C2C12 cells

The CLH addition did not ($p>0.05$) significantly affect cell survivability and LDH leakage in FL83B and C2C12 cells (Suppl. Fig. 1). Treatment with TNF-α reduced ($p<0.05$) glucose-uptake abilities in FL83B cells (30 ng TNF-α/mL) and C2Cl2 cells (20 ng TNF-α/mL) (Fig. 1A&C). An increased ($p<0.05$) glucose-uptake ability in FL83B and C2C12 cells was observed when the CLH supplementation exceeded 5 and 10 μg/mL, respectively (Fig. 1B&D). In terms of protein expressions related to IRβ-Akt-GSK3 pathway, TNF-α downregulated ($p<0.05$) IRβ, as well as ratios of p-GSK3/GSK3 in FL83B cells. However, these expressions in TNF-α treated FL83B cells were reversed ($p<0.05$) by supplementation with CLHs. In C2C12 cells, although TNF-α did not ($p>0.05$) decrease IRβ expression, the ratios of p-Akt/Akt and p-GSK3/GSK3 were reduced ($p<0.05$) by TNF-α treatment. Nonetheless, CLH supplementation upregulated ($p<0.05$) IRβ (> 5 μg/mL), as well as ratios of p-Akt/Akt (> 10 μg/mL) and p-GSK3/GSK3 (> 5 μg/mL) in TNF-α treated C2C12 cells.

Blood-glucose homeostasis, growth performance, organ, adipose tissue and hindlimb gastrocnemius tissue weight, and serum biochemical values of db/db mice

In the OGTT results, spontaneously diabetic db/db mice had higher serum glucose levels compared to Control mice (Fig. 2A). However, supplementation with CLHs or ACTOS reduced ($p<0.05$) glucose levels in db/db mice at each 30-min interval up to 120 min. Additionally, db/db group showed a fourfold increase in serum glucose AUC compared to the Control group (Fig. 2B). Notably, CLHs and ACTOS supplementation decreased ($p<0.05$) glucose AUC levels in db/db mice, but could not ($p>0.05$) reverse the levels to that of Control group. After a sacrifice, db/db group exhibited higher ($p<0.05$) serum glucose levels than Control group, but lower serum insulin levels were only assessed in db/db+CLH 2X and db/db+ACTOS groups ($p<0.05$) (Table 1). Serum glucose and HOMA-IR values in db/db mice were reduced ($p<0.05$) by supplementation of CLHs or ACTOS. Regarding the growth performance, db/db mice had the heavier ($p<0.05$) initial and final body weights than Control mice. Moreover, daily feed and water intakes were higher ($p<0.05$) in db/db mice than those in Control mice while CLH and ACTOS supplementation only decreased ($p<0.05$) the water intakes in db/db mice. With respect to organ weights, there were no ($p>0.05$) changes on weights of heart and spleen among groups. However, db/db mice had heavier ($p<0.05$) liver, kidney, and subcutaneous and abdominal (perirenal, mesenteric, and epididymal) adipose tissues than Control mice. Moreover, supplementation with CLHs reduced the weights of the liver and subcutaneous, abdominal (perirenal, mesenteric, and epididymal) adipose tissues in db/db mice. Specifically, the liver and epididymal adipose tissues showed significant reductions in the db/db+CLH 2X group compared to db/db controls ($p<0.05$), while reductions ($p<0.05$) in perirenal and mesenteric adipose tissues were observed in both CLH-supplemented groups. In contrast, ACTOS supplementation did not ($p>0.05$) affect liver or adipose tissue weights in db/db mice. In comparison with Control mice, the smaller ($p<0.05$) hindlimb gastrocnemius was observed in db/db mice. However, CLH or ACTOS supplementation increased ($p<0.05$) the gastrocnemius weight, although it remained lighter ($p<0.05$) than that of the Control group. In terms of serum biochemical values, db/db mice had higher ($p<0.05$) serum triglyceride, total cholesterol, AST, ALT levels, and DPP4 activity than Control mice. However, CLH or ACTOS supplementation reduced ($p<0.05$) these values in db/db mice but still higher ($p<0.05$) than those in Control mice, except DPP4 activities (db/db+CLH 2X and db/db+ACTOS vs. Control, $p>0.05$). Besides, the lower ($p<0.05$) serum GLP1 level was observed in db/db mice than that in Control group.

Table 2
Effects of CLHs on serum and liver antioxidant capacities, and liver inflammatory cytokine levels in experimental mice.

	Control	db/db	db/db+CLH 1X	db/db+CLH 2X	db/db+ACTOS
	Serum				
TBARS (nmole MDA eq./mL serum)	36.23 ±2.12d	199.17 ±10.01a	170.31 ±13.08b	117.62 ±10.46c	114.46 ±7.31c
TEAC (μmole/mL serum)	17.52 ±0.12a	14.74 ±0.12c	15.78 ±0.20a	15.58 ±0.13a	15.37 ±0.48bc
	Liver				
TBARS (nmole MDA eq./mg protein)	1.17 ±0.13c	2.38 ±0.12a	1.92 ±0.11b	1.31 ±0.18c	2.09 ±0.15ab
Reduced GSH (nmole/mg protein)	44.15 ±2.70a	28.65 ±3.35b	43.10 ±4.23a	45.75 ±3.78a	39.27 ±2.29a
TEAC (μmole/mg protein)	3.24 ±0.03a	0.96 ±0.04c	1.42 ±0.07b	1.55 ±0.12b	1.56±0.11b
SOD (unit/mg protein)	5.06 ±0.13b	4.36 ±0.26b	7.83 ±0.18a	8.32 ±0.34a	7.60±0.33a
Catalase (unit/mg protein)	86.38 ±2.57a	54.02 ±2.33d	68.35 ±2.84c	77.57 ±2.91b	68.48 ±2.59c
GPx (unit/mg protein)	4.23 ±0.16a	1.96 ±0.17c	3.33 ±0.24b	2.84 ±0.20b	2.84±0.19b
	Liver cytokines				
IL-1β (pg/mg protein)	286.10 ±23.08d	601.72 ±27.90a	408.44 ±26.01b	386.25 ±25.40bc	322.50 ±16.83dc
IL-6 (pg/mg protein)	134.93 ±7.31c	488.78 ±26.33a	328.95 ±31.20b	353.31 ±25.77b	359.80 ±34.83b
TNF-α (pg/mg protein)	185.27 ±18.68c	331.47 ±31.54a	293.16 ±32.70ab	237.34 ±29.00bc	193.77 ±21.80c

* Data are given as mean±SEM (n=8). Mean values without a common letter indicate a significant difference ($p<0.05$).

Conversely, 2X CLH supplementation normalized ($p<0.05$) the GLP-1 level in db/db mice to a level similar ($p>0.05$) to that of the Control mice.

Serum and liver antioxidant capacities, as well as liver cytokines

Table 2 demonstrates the serum and liver antioxidant status, as well as liver cytokine levels. The db/db group exhibited higher ($p<0.05$) serum TBARS values but lower ($p<0.05$) TEAC values compared to Control group. However, supplementation with CLHs or ACTOS reduced ($p<0.05$) serum TBARS values but still higher ($p<0.05$) than Control mice. Inspiringly, CLH supplementation elevated ($p<0.05$) serum TEAC values in db/db mice which were similar ($p>0.05$) to that of Control mice. In livers, the highest ($p<0.05$) TBARS value was measured in db/db group, following by db/db+ACTOS, db/db+CLH 1X, db/db+CLH 2X, and Control group. Conversely, db/db group had lower reduced GSH and TEAC values in livers compared to Control group. CLH or ACTOS supplementation enhanced ($p<0.05$) these two values in db/db mice, where the reduced GSH values in livers of db/db mice supplemented with CLHs or ACTOS were similar ($p>0.05$) to that of Control mice. With respect to antioxidant enzyme activities in livers, db/db group displayed unchanged ($p>0.05$) SOD activity and lower ($p<0.05$) catalase and GPx activities than Control group. However, supplementation with CLHs or ACTOS augmented ($p<0.05$) all 3 enzyme activities in db/db mice. Besides, db/db mice had higher ($p<0.05$) liver IL-1β, IL-6, and TNF-α levels than Control mice. Supplementation with CLHs significantly reduced ($p<0.05$) the levels of these cytokines in db/db mice, except TNF-α in the db/db+CLH 1X group ($p>0.05$). However, cytokine levels in CLH-supplemented db/db mice remained higher than those in Control mice ($p<0.05$), except for TNF-α in the db/db+ACTOS group ($p>0.05$).

Lipid contents in livers as well as glycogen contents in livers and hindlimb muscles

In the analyses of liver lipid contents (Table 1), the higher ($p<0.05$) levels of triglycerides and cholesterol were assessed in db/db group compared to the other groups, but there seem no ($p>0.05$) effects of ACTOS supplementation on elevated liver lipids of db/db mice. Conversely, supplementation with CLHs led to a significant reduction ($p<0.05$) in both triglyceride and cholesterol content in the liver of db/db mice, though the levels remained elevated ($p<0.05$) compared to those in the Control mice. Histological examination of liver tissues (Fig. 2C) revealed numerous and large lipid vacuoles in db/db groups, but these vacuoles were apparently reduced in the number and size in the CLH or ACTOS supplemented groups. This observation was also supported by the evaluation of steatosis score, with the highest score recorded in the db/db group, followed by db/db+ACTOS, db/db_CLH 1X, db/db+CLH 2X, and Control group (Fig. 2D).

In terms of glycogen disposition in liver tissues, PAS staining was used to detect glycogen, which appeared as pink or dark magenta color. Fig. 3A showed that db/db mice had more glycogen content indicated by yellow arrows in liver tissues compared to Control mice. Both CLH and ACTOS supplements apparently increased the glycogen content in livers of db/db mice. Moreover, db/db mice exhibited less glycogen deposition in hindlimb gastrocnemius tissues, marked by dot-circle areas, compared to Control mice (Fig. 3B). However, supplementation with CLHs or ACTOS increased glycogen contents in the hindlimb tissues of db/db mice.

Discussion

Among the 1.3 billion tons of waste generated annually in Europe, approximately 700 million tons come from agricultural residues or waste (Toop et al., 2017). On average, around 1,000 metric tons of broiler livers produced yearly after broilers are slaughtered (Ministry of Agriculture, Executive Yuan, Taiwan, 2023). This raises an urgent question: "What more can academia do to utilize broiler livers effectively?" in Taiwan. Protein hydrolysis offers a possible application for maximizing utilization and adding value to animal by-products (Wu and Chen, 2021). Several studies have shown on that the hydrolysates from animal by-product, for example, broiler livers, are used as a key ingredient in hepatoprotective products (Lin et al, 2023; Wu et al., 2024; Lin et al., 2024). The role of protein hydrolysates in stimulating post-exercise glycogen synthesis in skeletal muscle has been discussed (Manninen, 2009). Additionally, several amino acids, i.e. taurine (Inam-U-Llah et al., 2018), glycine (Li et al., 2019a), BCAAs (Zhu et al., 2021), and imidazole-ring dipeptides, i.e. anserine (Peters et al., 2018), have been proven to own a glucose-lowering effect. According to the analyses of free amino-acid profile and imidazole-ring dipeptide (Suppl. Table 1.), the contents of taurine, glycine, and BCAAs in CLHs are 437.13, 756.13, and 3048.10 mg/100g, respectively, while there is 164.50 mg anserine/100g. Hence, it has been proven that CLHs could lower blood glucose and ameliorate cognitive dysfunction in STZ induced mice (type I diabetes model) (Yeh et al., 2022). Type II diabetes, which accounts for 90% of cases, is primarily caused by insulin resistance, with the liver and muscles playing crucial roles in maintaining glucose homeostasis in response to insulin (Ahmad et al., 2022).

Several reports have shown that stimulating glycogenesis can decrease blood glucose levels (Li et al., 2019b; Zhu et al., 2021; Wang et al., 2022). TNF-α is a common agent to induce insulin resistance in liver or muscle cells (Huang et al., 2009; Lee et al., 2011). TNF-α could decrease insulin sensitivity and GLUT4 translocation by disrupting the insulin signaling pathway (de Alvaro et al., 2004). Specifically, TNF-α disrupts the insulin signaling pathway by impairing the

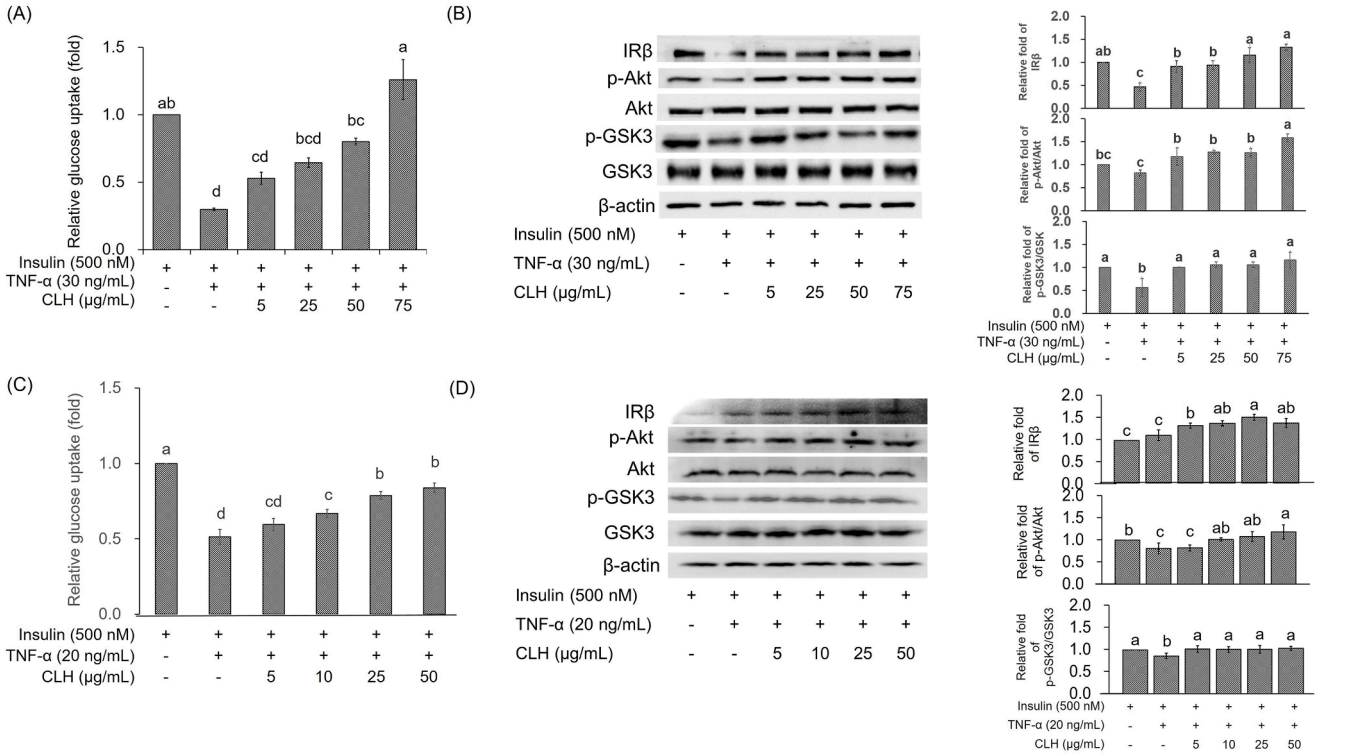

Fig. 1. Effects of CLHs on 2-DG uptake activity, and insulin receptor β (IRβ) protein expression and ratios of p-Akt/Akt and p-GSK3/GSK3 in TNF-α treated FL83B cells (A&B) and C2C12 cells (C&D).
* The data are given as mean±SEM (n=3). The data bars in each test parameter without a common letter indicate a significant difference ($p < 0.05$).

insulin-stimulated tyrosine phosphorylation of the IR and IR substrates-1 (IRS-1) and IRS-2, which affects IRS-associated activation of phosphatidylinositol 3-kinase and the subsequent phosphorylation of Akt. Additionally, insulin activates IRs, phosphorylated Akt, phosphorylated GSK, promoting glycogen synthesis by inactivating phosphorylated GSK3 (Petersen and Shulman, 2018). Consequently, insulin resistance downregulates the glycogenesis by disputing the IR-Akt-GSK3 pathways.

Our previous study indicated that CLH supplementation increases GLUT4 protein levels in the brain, liver, and hindlimb muscle of STZ induced mice (Yeh et al., 2022). *In vitro* data in this study showed that CLH supplementation reverse or even increase TNF-α induced reductions in IRβ protein expression in both FL83B cells (Fig. 1B) and C2C12 cells (Fig. 1D). These effects correlated with the increased the glucose uptake in TNF-α treated FL83B (Fig. 1A) and C2C12 cells (Fig. 1B) by supplementation with CLHs. In both liver and muscle cells, downregulated activations of Akt and GSK3 caused by TNF-α were also reversed by supplementation with CLHs (Fig. 1B&D), suggesting that the impaired glycogen synthesis in TNF-α treated cells can be mitigated by CLH supplementation. These reversed effects of glycogen synthesis also echoed the PAS-stained observations in liver and hindlimb tissues of db/db mice supplemented with CLHs (Fig. 3).

The oral glucose tolerance test and serum HOMA-IR value are commonly applied to detect the level of insulin resistance (Chen et al., 2021; Yeh et al., 2022). Our data demonstrated that db/db group was unable to lower serum glucose levels after an oral glucose gavage (Fig. 1A&B) and has the HOMA-IR value 3-times higher than that of Control group (Table 1). ACTOS, a hypoglycemic agent, has been shown to increase insulin sensitivity (Liu et al., 2020; Yeh et al., 2022). Several amino acids in CLHs, such as taurine (Inam-U-Llah et al., 2018), glycine (Li et al., 2019a), branched-chain amino acid (BCAA) (Zhu et al., 2021), and anserine (Peters et al., 2018), have hypoglycemic effects. ELDerawi et al. (2018) also reported that an improvement of magnesium (Mg) supplementation on the glycemic control indicators among type II patients is related to enhancing insulin sensitivity. These glucose-lowering effects were also observed in db/db mice (Fig. 1A&B and Table 1), likely due to the specific free amino acid (taurine: 437.13 mg /100 g; glycine: 756.13 mg/100 g; BCAA: 3048.10 mg/100 g), imidazole-ring dipeptide (anserine: 164.50 mg/100 g), and Mg (90 mg/Kg) (Suppl. Table 1), increased IRβ protein level, and upregulated glycogenesis pathways in liver and muscle (p-Akt and p-GSK expressions, Fig. 1B&D; PAS staining, Fig. 3), thus resulting in enhanced glucose uptake and insulin sensitivity in the liver and muscle (Fig. 1A&C).

The db/db mouse model arises from a spontaneous mutation of leptin receptor (a single autosomal recessive Gly-> Thr mutation), leading to severe obesity, hyperglycemia, polyphagia, polydipsia, and polyuria (Suriano et al., 2021). This model is widely used for type II diabetes and obesity. Similarly, the results in this study showed the higher ($p<0.05$) body weight, feed and water intakes, liver, body adipose tissues in db/db mice compared to Control mice (m^+/n^+ mice) (Table 1). Besides, the observations of higher glucose, insulin, triglyceride, total cholesterol, AST, ALT, and GLP1 levels in their sera of db/db mice are consistent with previous studies (Li et al., 2019b; Wang et al., 2020; Yang et al., 2020; Suriano et al., 2021). The physiological substrates of DPP4 include GLP1 and gastric inhibitory polypeptide (Zhong et al., 2015). These incretin hormones play crucial roles in glucose homeostasis by enhancing insulin secretion and suppressing glucagon release in response to nutrient intake. Furthermore, diabetic patients, particularly those with an insulin resistance, often experience muscle atrophy which results from downregulated GLUT4 and glycogenesis, increased muscle protein breakdown, enhanced oxidative stress, and impaired mitochondrial function (Abdulla et al., 2016; Rudrappa et al., 2016). Similarly, the reduced gastrocnemius weights of db/db mice were also observed in this study (Table 1). Moreover, an oxidative stress in type II diabetes was observed in serum and liver antioxidant capacities (Table 2). The liver lipid accumulation and inflammation were also elevated in db/db mice (Xue et al, 2018; Li et al., 2019b). The above

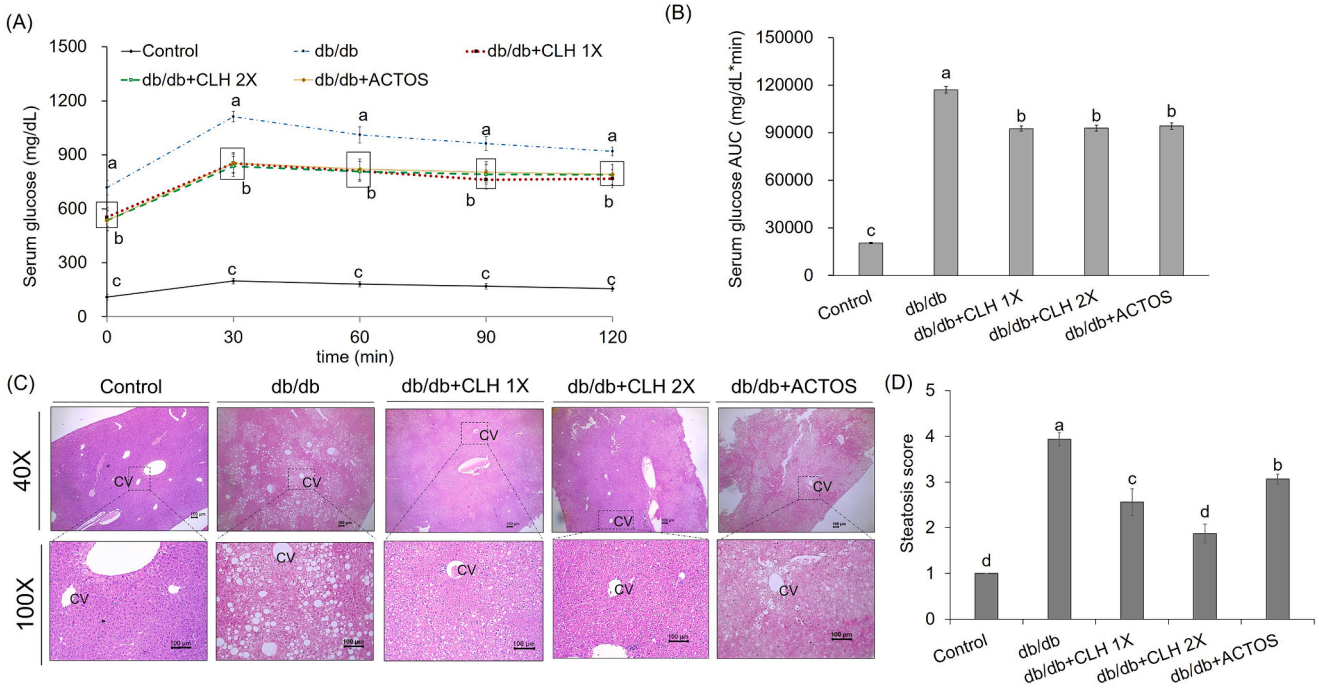

Fig. 2. Effects of CLHs on (A) oral glucose tolerance test, (B) blood glucose AUC, (C) H&E stained illustrations of liver tissues, and (D) the steatosis score of livers of the experimental mice.
* Data are given as mean±SEM (n=8). Data bars or data point at each test time without a common letter indicate a significant difference. ($p<0.05$).

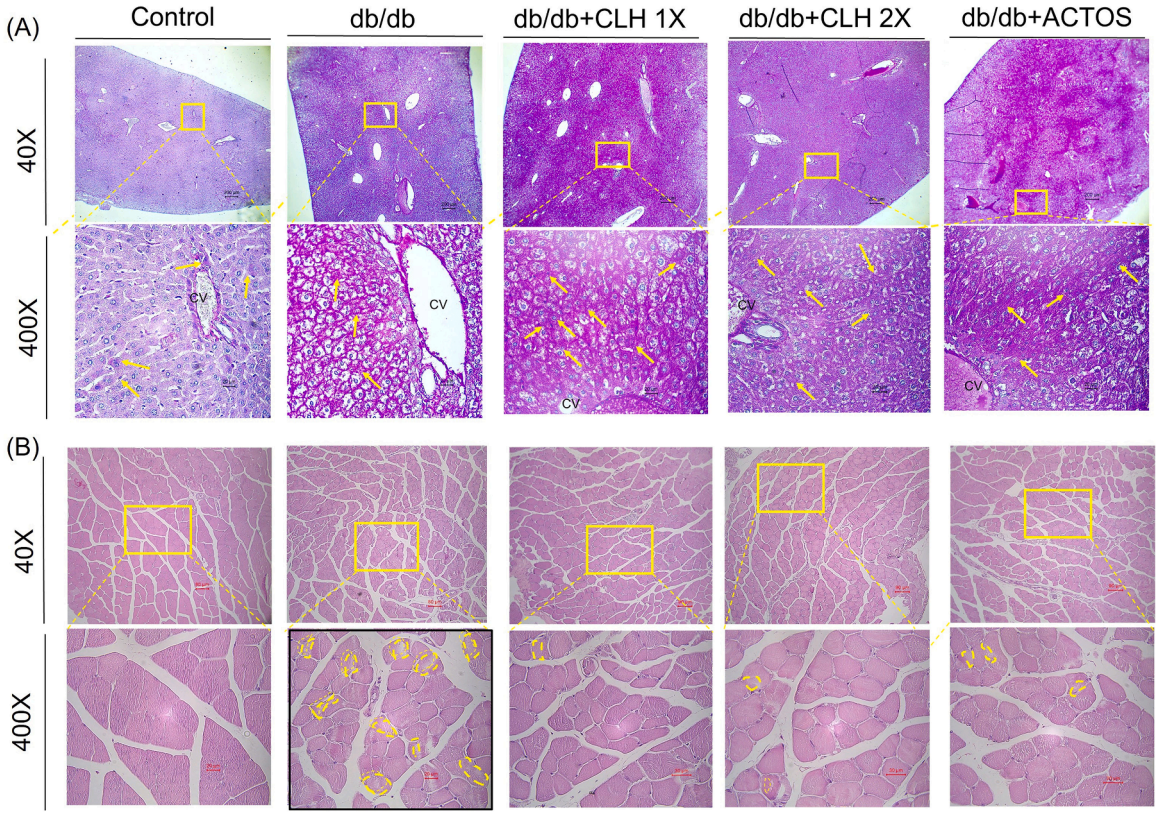

Fig. 3. Effects of CLHs on PAS stained illustrations for glycogen deposition in (A) liver and (B) hindlimb-gastrocnemius tissues of experimental mice.
* Yellow arrows in liver tissues indicate glycogen.
** Dot-circle areas indicates less or no glycogen accumulation.

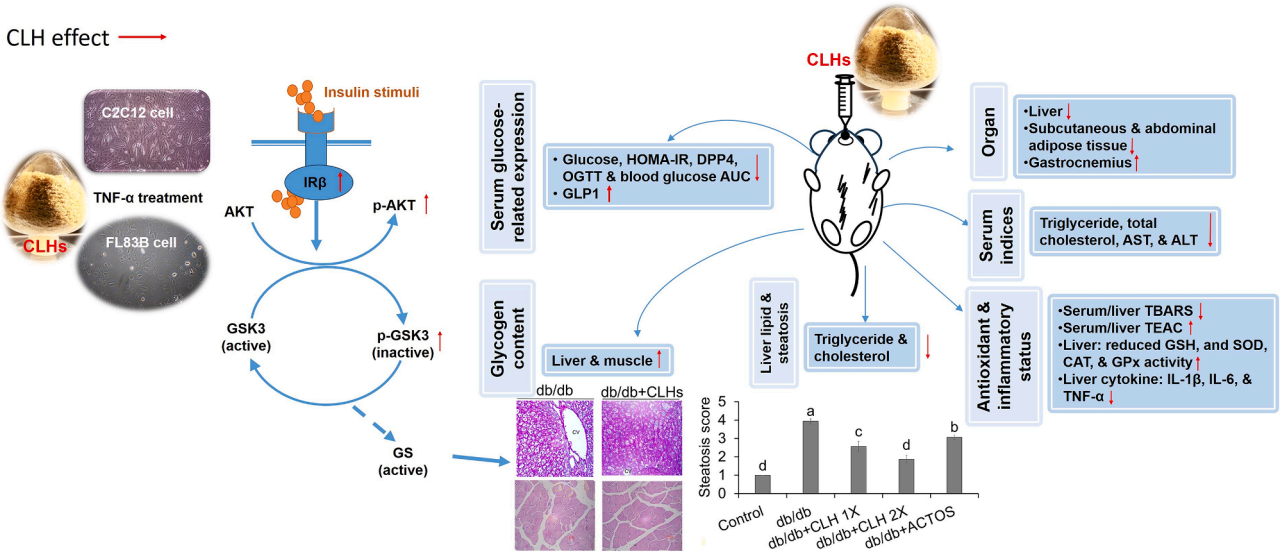

Fig. 4. Mitigation of CLHs on type II diabetes.

complications of db/db mice were also observed in this experiment (Table 1&2; Fig. 2).

Based on the several specific free amino-acid contents and imidazole-ring dipeptide (anserine) in CLHs, the lipid-lowering, antioxidative, hypoglycemic, and hepatoprotective effects of our CLHs against high-fat diets, alcohol consumption, and STZ induction were mentioned (Yang et al., 2014; Lin et al., 2017; Wu et al., 2020&2021; Yeh et al., 2022). The benefits of CLHs on lowering lipid and blood glucose levels in a long-term high-fat die result from downregulating fatty-acid synthesis and upregulating fatty-acid β oxidation in the liver, as well as increasing GLUT4 protein expressions in liver, skeletal muscle, and peri-renal adipose tissues (Wu et al., 2021). Based on the *in vitro* and *in vivo* data from this study, the amelioration of our CLHs against hyperglycemia and reduced muscle weight in type II diabetes (insulin resistance) could be attributed to increased glycogenesis in liver and muscle tissues through IRβ-Akt-GSK3 pathway and increased serum GLP1 level, which lower serum glucose and DPP4 activity and promote an insulin sensitivity (Table 1; Fig. 1, 2A, &B). The glycogen accumulation in livers and hindlimb tissues was also evidenced in db/db mice (Fig. 3). In addition to the specific free amino acid content and imidazole-ring dipeptides, CLHs contain Mn and Se (Suppl. Table 1), which are essential cofactors for SOD and GPx, respectively, and contribute to antioxidant effects (Chou et al., 2014). The antioxidant properties of CLHs have been shown to reduce inflammatory cytokines in the livers of mice fed an alcoholic diet (Lin et al., 2017) and rats with thioacetamide-induced liver fibrosis (Chen et al., 2017). Furthermore, CLH supplementation also demonstrated to alleviate oxidative stress and inflammation in the liver of db/db mice (Table 1 & 2; Fig. 2C & D).

Conclusion

This study demonstrates the potential of chicken-liver hydrolysates (CLHs) to alleviate type II diabetes *in vitro* (muscle and liver cells) and *in vivo* (db/db mice) (Fig. 4). In both cell types, insulin resistance was induced by TNF-α while CLH supplementation activated the IRβ-AKT-GSK pathway, enhancing glycogen production. In db/db mice, CLH supplementation improved blood glucose markers, including serum glucose, HOMA-IR, DPP4, blood glucose AUC, and GLP-1 while also reducing liver lipid levels and damage indices (AST and ALT) and proinflammatory cytokines (TNF-α, IL-1β, and IL-6). Obesity-related conditions, such as enlarged liver, excessive adipose tissue accumulation, and reduced antioxidant capacity, were alleviated by CLH supplementation, and hindlimb-muscle tissue mass were increased, too. Histological analyses revealed CLH supplementation results in higher glycogen contents in liver and muscle tissues as well as lower liver lipid accumulation in db/db mice. Considering the substantial volume of low-value broiler livers, this approach aligns with global agrocycle policies by optimizing the use of poultry slaughter residues.

CRediT authorship contribution statement

Yi-Ling Lin: Methodology, Investigation, Visualization, Writing – original draft. **Yu-Pei Chen:** Investigation, Visualization. **Sheng-Yao Wang:** Visualization, Validation, Writing – review & editing. **Yi-Feng Kao:** Visualization, Validation, Writing – review & editing. **Chompunut Lumsangkul:** Validation, Writing – review & editing. **Yi-Chen Chen:** Conceptualization, Investigation, Writing – review & editing, Supervision, Project administration, Funding acquisition.

Declaration of competing interest

The authors declare that they have no known competing financial interests or personal relationships that could have appeared to influence the work reported in this paper.

Acknowledgments

This research was partially by National Science and Technology Council, Taiwan (Project: MOST 109-2313-B-002-007-MY3, NSTC 113-2313-B-002-047-MY3, and NSTC 113-2221-E-002-032-MY3), Ministry of Agriculture, Taiwan (113AS -2.1.7-AD-01(1) and 113AS-15.2.2-AD-02), and Great Billion Biotech, Co., Ltd. (New Taipei City, Taiwan).

Supplementary materials

Supplementary material associated with this article can be found, in the online version, at doi:10.1016/j.psj.2024.104517.

References

Abdulla, H., Smith, K., Atherton, P.J., Idris, I., 2016. Role of insulin in the regulation of human skeletal muscle protein synthesis and breakdown: a systematic review and meta-analysis. Diabetologia 59, 44–55.

Ahmad, E., Lim, S., Lamptey, R., Webb, D.R., Davies, M.J., 2022. Type 2 diabetes. Lancet 400, 1803–1820.

Chadt, A., Al-Hasani, H., 2020. Glucose transporters in adipose tissue, liver, and skeletal muscle in metabolic health and disease. Pflüg. Arch. Eur. J. Physiol. 472, 1273–1298.

Chen, P.J., Tseng, J.K., Lin, Y.L., Wu, Y.H.S., Hsiao, Y.Y., Chen, J.W., Chen, Y.C., 2017. Protective effects of functional chicken liver hydrolysates against liver fibrogenesis: Antioxidation, anti-inflammation, and antifibrosis. J. Agric. Food Chem. 65, 4961–4969.

Chen, Y.C., Chen, P.J., Tai, S.Y., 2018. Composition of Chicken Liver Hydrolysates and Method for Improving Alcohol Metabolism, as Well as Preventing and Treating Liver Fibrosis. National Taiwan University, Assignee. USA patent: US10,105,400B2. Oct. 23, 2018.

Chen, J.W., Lin, Y.L., Chou, C.H., Wu, Y.H.S., Wang, S.Y., Chen, Y.C., 2020. Antiobesity and hypolipidemic effects of protease A-digested crude-chalaza hydrolysates in a high-fat diet. J. Funct. Food 66, 103788.

Chen, J.W., Lin, Y.L., Wu, Y.H.S., Wang, S.Y., Chou, C.H., Chen, Y.C., 2021. Ameliorative effects of functional crude-chalaza hydrolysates on the hepatosteatosis development induced by a high-fat diet. Poult. Sci. 100, 101009.

Chen, Y.C., Yeh, W.Y., Lin, Y.L., Wu, Y.H.S., Chen, Y.C., 2022. Use of Chicken-Liver Hydrolysates for Manufacturing Composition for Improving Diabetes and Cognitive Dysfunction (In Chinese). Great Billion Biotech Co., Ltd., Investor. New Taipei City, Taiwan, assignee. Taiwan Patent: I777515.

Chou, C.H., Wang, S.Y., Lin, Y.T., Chen, Y.C., 2014. Antioxidant activities of chicken liver hydrolysates by pepsin treatment. Int. J. Food Sci. Technol. 49, 1654–1662.

de Alvaro, C., Teruel, T., Hernandez, R., Lorenzo, M., 2004. Tumor necrosis factor alpha produces insulin resistance in skeletal muscle by activation of inhibitor kappaB kinase in a p38 MAPK-dependent manner. J. Biol. Chem. 279, 17070–17078.

Dixon, J.B., Bhathal, P.S., Hughes, N.R., O'Brien, P.E., 2004. Nonalcoholic fatty liver disease: improvement in liver histological analysis with weight loss. Hepatology 39, 164.

ELDerawi, W.A., Naser, I.A., Taleb, M.H., Abutair, A.S., 2018. The effects of oral magnesium supplementation on glycemic response among type 2 diabetes patients. Nutrients 11, 44.

Furman, B.L., 2021. Streptozotocin-induced diabetic models in mice and rats. Curr. Protoc. 1, e78.

Huang, D.W., Shen, S.C., Wu, J.S.B., 2009. Effects of caffeic acid and cinnamic acid on glucose uptake in insulin-resistant mouse hepatocytes. J. Agric. Food Chem. 57, 7687–7692.

Huang, D.W., Chang, W.C., Wu, J.S.B., Shih, R.W., Shen, S.C., 2016. Gallic acid ameliorates hyperglycemia and improves hepatic carbohydrate metabolism in rats fed a high-fructose diet. Nutr. Res. 36, 150–160.

Inam-U-Llah, P.P., Aadil, R.M., Suleman, R., Li, K., Zhang, M., Wu, P., Shahbaz, M., Ahmed, Z., 2018. Ameliorative effects of taurine against diabetes: a review. Amino Acids 50, 487–502.

Lee, B.H., Hsu, W.H., Liao, T.H., Pan, T.M., 2011. The Monascus metabolite monascin against TNF-α-induced insulin resistance via suppressing PPAR-γ phosphorylation in C2C12 myotubes. Food Chem. Toxicol. 49, 2609–2617.

Li, W., Zhang, Y., Shao, N., 2019a. Protective effect of glycine in streptozotocin-induced diabetic cataract through aldose reductase inhibitory activity. Biomed. Pharmacother. 114, 108794.

Li, J., Zhao, H., Hu, X., Shi, J., Shao, D., Jin, M., 2019b. Antidiabetic effects of different polysaccharide fractions from *Artemisia sphaerocephala* Krasch seeds in db/db mice. Food Hydrocolloid 91, 1–9.

Liao, W., Cao, X., Xia, H., Wang, S., Chen, L., Sun, G., 2023. Pea protein hydrolysate reduces blood glucose in high-fat diet and streptozotocin-induced diabetic mice. Front. Nutr. 10, 1298046.

Lin, Y.L., Tai, S.Y., Chen, J.W., Chou, C.H., Fu, S.G., Chen, Y.C., 2017. Ameliorative effects of pepsin-digested chicken liver hydrolysates on development of alcoholic fatty livers in mice. Food Funct 8, 1763–1774.

Lin, Y.L., Chen, C.Y., Yang, D.J., Wu, Y.H.S., Lee, Y.J., Chen, Y.C., Chen, Y.C., 2023. Hepatic-modulatory effects of chicken liver hydrolysate-based supplement on autophagy regulation against liver fibrogenesis. Antioxidants 12, 493.

Lin, Y.L., Cheng, K.C., Kao, Y.F., Wu, K., Chen, J.W., Nakthong, S., Chen, Y.C., 2024. Valorization of broiler edible byproducts: a chicken-liver hydrolysate with hepatoprotection against binge drinking. Poult. Sci. 103, 104023.

Liu, T.H., Lin, W.J., Cheng, M.C., Tsai, T.Y., 2020. *Lactobacillus plantarum* TWK10-fermented soymilk improves cognitive function in type 2 diabetic rats. J. Sci. Food Agric. 100, 5152–5161.

Lu, J.M., Wang, Y.F., Yan, H.L., Lin, P., Gu, W., Yu, J., 2016. Antidiabetic effect of total saponins from *Polygonatum kingianum* in streptozotocin-induced diabetic rats. J. Ethnopharmacol. 179, 291–300.

Manninen, A.H., 2009. Protein hydrolysates in sports nutrition. Nutr. Metab. 6, 1–5.

Ministry of Agriculture, Executive Yuan, Taiwan. 2023. Yearly report of Taiwan's agriculture. 2022. Agriculture Production. 2. Livestock Production. Available: https://eng.moa.gov.tw/upload/files/eng_web_structure/2505724/2-3%E7%95%9C%E7%89%A7%E7%94%9F%E7%94%A2111(%E9%83%A8).pdf (Accessed date: 2024/9/8).

Ministry of Health and Welfare, Taiwan. 2023. Statistics. Cause of death statistics. Available: https://dep.mohw.gov.tw/DOS/lp-5069-113-xCat-y110.html (In Chinese) (Accessed date: 2024/9/9).

Park, S., Jevtovic, F., Krassovskaia, P.M., Chaves, A.B., Zheng, D., Treebak, J.T., Houmard, J.A., 2020. Effect of resveratrol on insulin action in primary myotubes from lean individuals and individuals with severe obesity. Am. J. Physiol. Endocrinol. Metab. 326, E398–E406.

Peters, V., Calabrese, V., Forsberg, E., Volk, N., Fleming, T., Baelde, H., Weigand, T., Thiel, C., Trovato, A., Scuto, M., Modafferi, S., Schmitt, C.P., 2018. Protective actions of anserine under diabetic conditions. Int. J. Mol. Sci. 19, 2751.

Petersen, M.C., Shulman, G.I., 2018. Mechanisms of insulin action and insulin resistance. Physiol. Rev. 98, 2133–2223.

Rudrappa, S., Wilkinson, D.J., Greenhaff, P.L., Smith, K., Idris, I., Atherton, P.J., 2016. Human skeletal muscle disuse atrophy: Effects on muscle protein synthesis, breakdown, and insulin resistance- a qualitative review. Front. Physiol. 7, 361.

Suriano, F., Vieira-Silva, S., Falony, G., Roumain, M., Paquot, A., Pelicaen, R., Régnier, M., Delzenne, N.M., Raes, J., Muccioli, G.G., Van Hul, M., Cani, P.D., 2021. Novel insights into the genetically obese (*ob/ob*) and diabetic (*db/db*) mice: two sides of the same coin. Microbiome 9, 147.

Toops, T.A., Ward, S., Oldfield, T., Hull, M., Kirby, M.E., Theodorou, M.K., 2017. AgroCycle–developing a circular economy in agriculture. Energy Procedia 123, 76–80.

Wang, L., Li, J., Di, L.J., 2022. Glycogen synthesis and beyond, a comprehensive review of GSK3 as a key regulator of metabolic pathways and a therapeutic target for treating metabolic diseases. Med. Res. Rev. 42, 946–982.

Wu, Y.H.S., Lin, Y.L., Huang, C., Chiu, C.H., Nakthong, S., Chen, Y.C., 2020. Cardiac protection of functional chicken-liver hydrolysates on the high-fat diet induced cardio-renal damages via sustaining autophagy homeostasis. J. Sci. Food Agric. 100, 2443–2452.

Wu, Y.H.S., Lin, Y.L., Yang, W.Y., Wang, S.Y., Chen, Y.C., 2021. Pepsin-digested chicken-liver hydrolysate attenuates hepatosteatosis by relieving hepatic and peripheral insulin resistance in long-term high-fat dietary habit. J. Food Drug Anal. 29, 375–388.

Wu, Y.H.S., Chen, Y.C., 2022. Trends and applications of food protein-origin hydrolysates and bioactive peptides. J. Food Drug Anal. 30, 172–184.

Wu, Y.H.S., Lin, Y.L., Kao, Y.F., Chen, J.W., Chen, Y.C., Chen, Y.C., 2024. A functional chicken-liver hydrolysate-based supplement ameliorates alcohol liver disease via regulation of antioxidation, anti-inflammation, and anti-apoptosis. Environ. Toxicol. 39, 1759–1768.

Xue, W., Fan, Z., Li, Y., Li, L., Zhang, T., Lu, J., Ma, B., Zhu, Z., Lian, J., Zhang, C., Song, X., Sun, D., Zhai, Y., Fan, R., Cao, Y., Deng, X., Zhao, J., 2018. Alkannin inhibited hepatic inflammation in diabetic db/db mice. Cell. Physiol. Biochem. 45, 2461–2470.

Yang, K.T., Lin, C., Liu, C.W., Chen, Y.C., 2014. Effects of chicken-liver hydrolysates on lipid metabolism in a high-fat diet. Food Chem 160, 148–156.

Yang, T., Yang, H., Heng, C., Wang, H., Chen, S., Hu, Y., Jiang, Z., Yu, Q., Wang, Z., Qian, S., Wang, J., Wang, T., Du, L., Lu, Q., Yin, X., 2020. Amelioration of non-alcoholic fatty liver disease by sodium butyrate is linked to the modulation of intestinal tight junctions in db/db mice. Food Funct 11, 10675–10689.

Yeh, W.Y., Lin, Y.L., Yang, W.Y., Chou, C.H., Wu, Y.H.S., Chen, Y.C., 2022. Functional chicken-liver hydrolysates ameliorate insulin resistance and cognitive decline in streptozotocin-induced diabetic mice. Poult. Sci. 101, 101887.

Zhong, J., Maiseyeu, A., Davis, S.N., Rajagopalan, S., 2015. DPP4 in cardiometabolic disease: Recent insights from the laboratory and clinical trials of DPP4 inhibition. Circ. Res. 116, 1491–1504.

Zhu, X., Wang, W., Cui, C., 2021. Hypoglycemic effect of hydrophobic BCAA peptides is associated with altered PI3K/Akt protein expression. J. Agric. Food Chem. 69, 4446–4452.